ACS Partner Journal

Journal of the American Society for Mass Spectrometry

pubs.acs.org/jasms

Research Article

Gigaohm and Teraohm Resistors in Femtoamp and Picoamp Electrospray Ionization

Published as part of the Journal of the American Society for Mass Spectrometry virtual special issue "Focus: Ion Chemistry and Electrospray Ionization".

Nicholas Allen, Huishan Li, Taoqing Wang, and Anyin Li*

Cite This: *J. Am. Soc. Mass Spectrom.* 2023, 34, 913−921

Read Online

ACCESS | Metrics & More | Article Recommendations | Supporting Information

ABSTRACT: The femtoamp electrospray ionization (femtoESI) mode has been shown to exhibit unique characteristics that may facilitate ionization efficiency studies and experiments requiring low ion beam flux. Investigation of femtoESI was hindered by a tiny, applied voltage window of 10−100 V, beyond which ionization currents quickly jumped to nanoamps. This window was difficult to locate because the exact onset voltage fluctuates due to variations in ion source alignments. Large resistors (0.1−100 TΩ) in series effectively expanded the femtoESI applied voltage range, up to 1400 V. By swapping resistors, rapid alternation allows for the comparison of both ESI modes under the same alignment. In peptide mixtures, analytes with lower surface activity are suppressed in the nanoESI mode whereas the femtoESI mode shows signal enhancement of less surface-active species. For protein solutions, there is little change in the charge states generated but the femtoESI mode does show a decrease in the average charge state of protein peaks. Peptides and proteins analyzed in the femtoESI mode also tend to generate higher intensity sodiated peaks over protonated peaks at specific charge states compared with nanoESI mode operation.

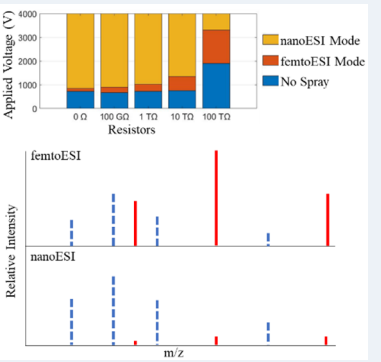

KEYWORDS: *electrospray, ionization current, nanoelectrospray, femtoelectrospray, ionization efficiency, nonspecific adduct*

INTRODUCTION

The ionization current associated with an electrospray ionization (ESI) emitter is one indicator of performance and the characteristics of the ESI process and yields insight into ion formation and predictions of charged droplet size.[1] The previously reported femtomode of ESI (femtoESI) delivers a low current ion beam for analysis by mass spectrometry.[2−4] The femtoESI mode previously suffered from a narrow applied voltage range where femtoESI signals are achieved. To achieve a more facile generation of the femtoESI mode signal over a broad range of applied voltages, a circuit scheme utilizing large resistors is used. Previous studies using tip-ESI with large resistors have demonstrated that using high-ohmic resistors (10 GΩ) greatly reduced ESI current, resulting in improved signal stability and avoidance of corona discharge, and that mass spectra can be obtained with tip sizes as large as 120 μm (internal diameter).[5] Small initially charged droplets have been shown to reduce the likelihood of dimer formation and improve ionization efficiency of mixtures.[3,6−13] The concentration and pH changes caused by evaporation increase with smaller droplets size and can also alter the conformations of proteins contained in the droplets.[13−16] With sufficiently small initial charged droplet size, Rayleigh fission events become increasingly less favorable and only droplet evaporation to dryness can occur, imparting more of the droplet charge onto the analyte when ion formation occurs and increasing the likelihood of ionization.[8,17] The generation of smaller charged droplets is also correlated with a decrease in the flow rate, the surface tension of sample solution, and spray current.[11,18] Flow rates for the femtoESI mode are estimated in the single fL/min range (below the solutions evaporation rate) using the Pfeifer/Hendricks' equation and the solution parameters at femtoESI onset.[18,19]

Ionization efficiency (IE) is a measure of the ratio of analyte(s) in solution which become charged and detected in the electrospray ionization mass spectrometry (ESI-MS) process. In analyte mixtures, one analyte will typically be more competitive for obtaining charge and thus suppresses other analytes in the mixture.[20,21] IE is affected by numerous factors such as liquid flow rate, solvent composition, geometry of the emitter, solution pK_a, amino acid composition, and chemical/physical properties of the analyte.[10,14,21−26] Generally, IE of mixtures is found to improve as a function of

Received: December 19, 2022
Revised: March 30, 2023
Accepted: April 4, 2023
Published: April 13, 2023

decreasing flow rate to the ESI emitter due to the formation of smaller initially charged droplets.[12] Smaller initial droplets and increased amount of charge available per analyte molecule also improve the ionization of analytes with lower surface activity, improve quantitation, and reduce matrix suppression effects.[27] The surface activity of an analyte is important for ionization efficiency due to the charge of a droplet residing on the surface, while the interior of the droplet is electrically neutral with a balance of cations and anions.[28]

In this study, the femtoESI scheme will be improved using large resistors to expand the applied voltage range at which the femtomode is achieved. The large resistors have been utilized in other studies for the purpose of limit the current to the glass capillary.[5,29] This expanded applied voltage range will be used to further characterize the femtoESI mode by exploring the impacts of the mode's unique performance on analyte charging, especially in analyte mixtures.

EXPERIMENTAL SECTION

Mass Spectrometer Measurements. Linear ion trap and Orbitrap mass spectrometers (LTQ-XL, LTQ velos Orbitrap mass spectrometer, Thermo Fisher, San Jose) were operated with the following parameters: inlet capillary voltage of 41 V, tube lens voltage of 0 V, and the inlet capillary temperature was set at 125−150 °C. The mass spectrometer method consisted of positive mode scans unless otherwise stated. The automatic gain control (AGC) target value is assigned as 3E4 with the maximum injection time (IT) varying with experiment from 0.002 to 8000 ms. Mass spectra were recorded and processed in Xcalibur Qual Browser (Thermo Fisher, San Jose) as peak profiles with one microscan. The ion sources were open to lab air unless stated otherwise, which had typical relative humidity ranging from 10% to 60%, and temperature was maintained at 20−25 °C from winter to summer.

Current Measurements. The voltage was applied and read using a DC high voltage power supply (model PS350, Stanford Research Systems, Inc., Sunnyvale, CA) applied through a resistor (Ohmite thick film resistors (10 GΩ to 100 TΩ), Mouser Electronics, Mansfield, TX) to a gold wire (0.1 mm diameter, 99.998%, Premion) electrode inserted directly into borosilicate glass capillaries in contact with the sample solution (B150-86-10, lot 190934, Sutter Instrument Co., Navato, CA) pulled by a micropipette puller (model P-1000, Sutter Instrument Co., Navato, CA) with a trough filament pulled to an outer diameter (o.d.) of 3−4 μm. The current was measured using a counter electrode (2.5 cm × 2.5 cm copper tape square) connected to an electrometer (Keithley 6514, Cleveland, OH) at a tip-to-electrode distance of ∼10 mm. The analog output of the electrometer was recorded directly from the electrometer screen by the user in five replicates (to obtain averaged and deviation values as well as smoothing out unstable femtoESI signal) or by a home-built LabVIEW (National Instruments, Austin, TX) program with a sampling frequency at 100 or 1000 Hz. All low current measurements were conducted inside a home-built faraday cage (0.03 Ω, copper + nickel + polyester, NVSUNG) to reduce the background noise magnitude. The DC bias, which varied from ∼10 to 50 fA, was recorded as a baseline to determine when femtoESI mode has been established and produces signal approximately 3× higher than background noise and is included when using a logarithmic scale.

Chemicals. Tetraethylammonium chloride (T2265), tetrahexylammonium chloride (263834), cytochrome *c* (C2506), melittin (M2272), bradykinin (B3259), angiotensin I (A9650), angiotensin II (A9525), neurotensin (N6383), substance P (S6883), ammonium acetate (A1542), sodium chloride (S9888), and methanol (34860-4L-R, HPLC grade) were purchased from Sigma-Aldrich (St. Louis, MO). Water (Pierce 51140, HPLC grade) was purchased from Fisher Scientific (Waltham, MA). Vancomycin (QR14945) was purchased from MP Biomedicals (Santa Ana, CA). Further information on solution preparation can be found in the Supporting Information.

Resistors. Details for Ohmite through hole thick film resistors purchased from Mouser Electronics (voltage rating, tolerance): 10 TΩ (30 kV, 10%), 1 TΩ (30 kV, 5%), 100 GΩ (30 kV, 5%), and 10 GΩ (10 kV, 5%). 100 TΩ resistor (30 kV, 1.96%): more information is in Supporting Information.

Additional information regarding the ESI emitters manufacturing and specifications used in this paper can be found in the Supporting Information.

RESULTS AND DISCUSSION

Characterization of the femtoESI Mode. Characterization of the influence of large resistors (0.1−100 TΩ) on the femtoESI mode was conducted by assembling the necessary circuitry and equipment to apply and read applied high voltage, low current signals and allow for alternation between the femtoESI and nanoESI modes. It is worth noting that the reported voltages are the "Applied Voltage" from the power supply, not the actual voltage at the emitter tip.

To better understand the phenomenon of femtoESI, the current produced by the ESI source must be characterized. This is undertaken using a grounded Faraday cage and shielded cables described in our previous work to lower the magnitude of background noise from the surrounding environment and the electrometer's internal noise to a level lower than the femtoESI currents (∼10−50 fA background) (Figure 1).[3] Without the use of a Faraday cage, the background noise can be on the order of single to tens of picoamperes, too high to measure fA currents. The current measurement apparatus is utilized to characterize the femtoESI mode by generating a current−applied voltage (*I*−*V*) curve by scanning applied voltage values and measuring current values. Collecting *I*−*V*

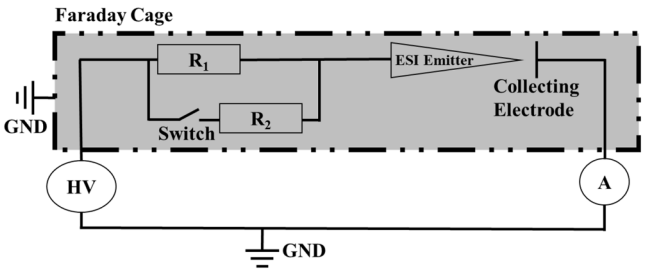

Figure 1. Circuit scheme for the current regulation during electrospray ionization. The high voltage source (HV) generates the potential difference and passes a voltage to the resistor (R_1). R_1 is the regulating resistor (0.1−100 TΩ) connected in series with the ESI emitter and aids in regulating the current experienced by the emitter. The circuit also contains a switch to bypass the resistor and allow for spraying through an alternate resistor (R_2, 0−10 MΩ) to generate nanoESI. The ESI emitter sprays onto a counter electrode where the current is measured by an electrometer (A). Current measurements are made within a grounded Faraday cage to reduce background noise.

https://doi.org/10.1021/jasms.2c00369
J. Am. Soc. Mass Spectrom. 2023, 34, 913−921

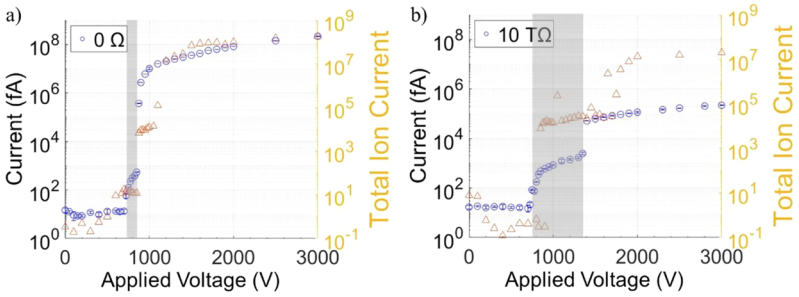

Figure 2. The log plots of $I-V$ (blue circle) and TIC$-V$ (orange triangle) behavior of an aqueous 10 μM equimolar mixture of tetraethylammonium chloride (TethylA) and tetrahexylammonium chloride (ThexylA). The solution was evaluated for two resistors (a) 0 Ω and (b) 10 TΩ. Current and TIC measurements are conducted independently with the same emitter and solution. Gray highlighted regions indicate the femtoESI mode current range.

curves for varying resistance shows that the range of applied voltage values at which previously described characteristic femtoESI currents (~50 fA to 1s pA) are observed expands with increasing resistance (Figures 2, S4, and S6). At a resistance of 0 Ω, the applied voltage range for femtoESI is 100 V (750−850 V) (Figure 2a). When increasing the value of the resistor up to 10 TΩ, the applied voltage window for femtoESI increases to 600 V (750−1350 V) (Figure 2b).

The increase in the femtoESI applied voltage range is attributed to the increasing resistance introducing a larger voltage drop across the resistor before the ion source. This voltage drop decreases the voltage felt by the emitter tip for a given current which allows for an expansion of the applied voltage range via more precise voltage scanning for femtoESI currents.

Figure 2 shows that similar trends are obtained for both current (I) and total ion current (TIC) versus applied voltage (V) curves. These TIC−V curves represent the total number of ions per scan recorded by the detector of the mass spectrometer at a given applied voltage value. The 0 Ω resistor (Figure 2a, Table S5) shows an onset of 750 V with a current of 123.6 ± 10.1 fA. The femtoESI region increases with added applied voltage to 850 V where the current rises to 542.2 ± 13.5 fA. This yields a total femtoESI applied voltage window of 100 V; TIC data roughly align with the current data reporting a femtoESI mode window of 250 V. It is also worth noting here that there appear to be two different operating modes in the TIC$-V$ curve as well. The lower TIC of these two sections (750−850 V) lies in a lower TIC range (10^1 ions) than mass spectrum signals for the other four resistors and has a more stable spray signal where the TethylA ion is completely suppressed, heavily favoring the larger, more nonpolar, ThexylA ion (Figure S7 top). The higher TIC data region (875−1050 V) in Figure 2a represents a sub-nanoESI pulsing mode which produces high ion currents at a lower duty cycle which averages to signals lower than typical nanoESI operation (Figure S7 bottom) and lies in the same TIC range (10^4 ions) per scan. This sub-nanoESI pulsing mode is also difficult to obtain and requires precise voltage scanning; the applied voltage range is also expanded with increasing resistance, allowing for some characterization of these pulsing modes (Figures S10 and S11). For the 10 TΩ resistor, the current is observed to be continuous (at a sampling rate of 1000 Hz) in the femtoESI mode, but at 3000+ V, there is a pulsing mode yielding single nA pulses with a duty cycle on the order of seconds where the duty cycle shortens with increasing applied voltage. Also, for the first time a pA pulsing regime was observed with a 10 s duty cycle and pulse heights of 49.4 pA (Figure S11).[30,31]

For the evaluation of the 10 TΩ resistor (Figure 2b, Table S5), $I-V$ and TIC$-V$ behavior also indicate an onset at 750 V with a current of 82.6 ± 2.8 fA and an end point at 1350 V, 2470 ± 250 fA. The nanoESI region begins at 1400 V where there is a break in continuity in the current, which jumps to 51.3 ± 0.8 pA. This yields a total femtoESI applied voltage window of 600 V; TIC data align with the current range with a femtoESI mode window of 750 V range. When increasing the applied voltage to the upper end of the femtoESI mode, the total intensity for both current and TIC greatly increases and some of the shorter carbon chain TethylA ion is observed in the spectrum (Figure S8 bottom). The variation in the exact onset voltage and the values of the applied voltage range are likely due to the variation in alignment when transitioning from the current apparatus to the MS. Increased applied voltage range for TIC values is attributable to the higher sensitivity of the mass spectrometer detector. The exact onset values and spray current will depend on the tip-to-electrode distance and tip geometry. Charged droplets are likely ejected from certain nanoscale edges of the emitter tip, analogous to those in probe electrospray ionization (PESI) experiments (Figures S1 and S2).[1,10,32,33]

Examining the femtoESI more closely, the current values behave differently during the beginning and the end of the applied voltage scanning within the mode. Current values tend to change the most rapidly when entering new modes (no spray to femtoESI and femtoESI to nanoESI) and increase asymptotically when a mode has been established (Figures 2, S4, and S6).

There is also a trend observed for the overall intensities in the current and TIC values. Not only is the applied voltage range where femtoESI signal is observed expanded when a larger resistor (0.1−100 TΩ) is used in the circuit, but the overall intensity up to 4000 V (the largest applied voltage used) is also decreased while still producing nanoESI characteristic spectra (Figures 2, S4, and S6). This means that even when the emitter is operating in the nanoESI regime, the overall current and TIC signals are lower than the 0 Ω resistor. For the 0 Ω resistor, at an applied voltage of 2000 V the current is 81 nA (TIC, 9.81E7), but when a 10 TΩ resistor is used, an applied voltage of 2000 V yields a current of 115 pA (TIC, 1.33E7) where both operate with nanoESI like mass spectra. There are an apparent 3 orders of magnitude decrease in the observed current under the larger resistor (0.1−100 TΩ) and a decrease in TIC with larger resistance.

https://doi.org/10.1021/jasms.2c00369
J. Am. Soc. Mass Spectrom. 2023, 34, 913−921

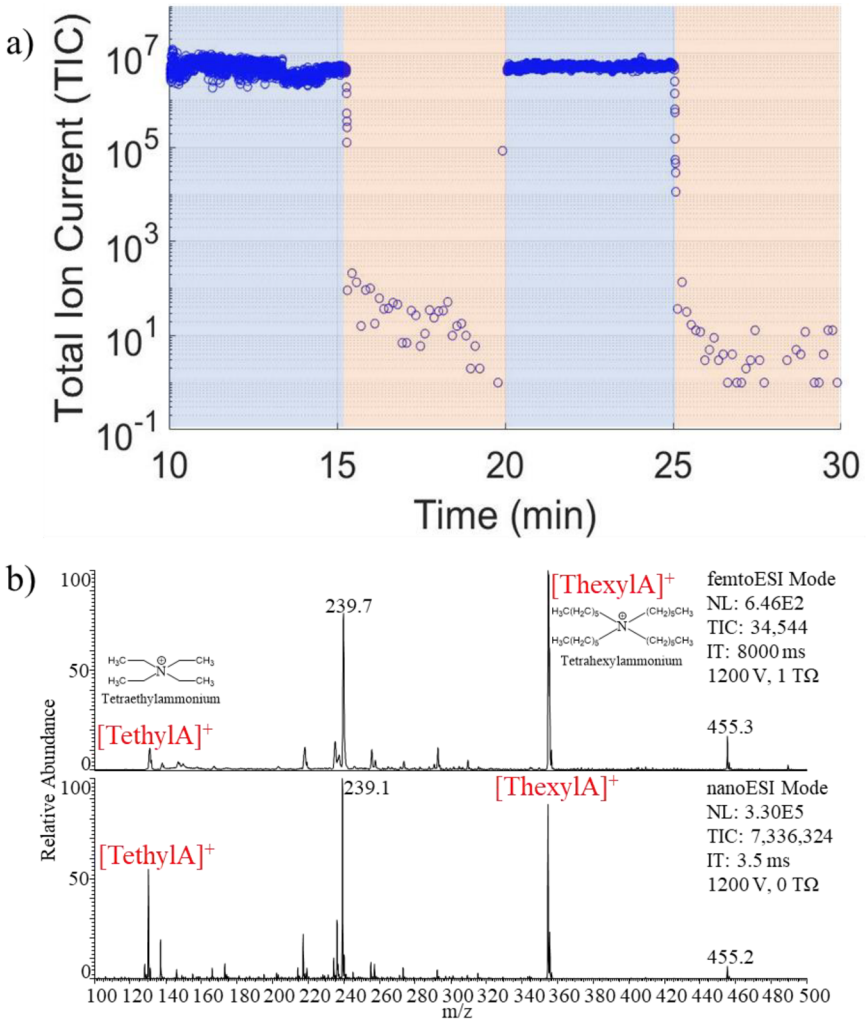

Figure 3. (a) TIC versus time plot with a log *y*-axis for an aqueous equimolar solution of TethylA and ThexylA alternating between 0 Ω and 1 TΩ at 1200 V. The data are presented as a moving average of 10 data points for smoothing purposes. Shaded sections indicate the nanoESI mode (blue) and the femtoESI mode (orange). (b) Mass spectrum for the femtoESI (top) and nanoESI (bottom) modes analyzing the equimolar mixture.

femtoESI Effects on Ion Formation and Detection. *Ionization of Small Organics.* Operation of the scheme shown in Figure 1 allows for the alternation between the two modes (femtoESI/nanoESI) by operating a switch in the circuit (Figure 3). This scheme allows for conducting experiments in the femtoESI mode to perform low ion current experiments while still having the option of performing high signal intensity experiments with a simple switch.

In the nanoESI mode (Figure 3b bottom), the equimolar mixture of two analytes shows an affinity toward the ionization of the more nonpolar ThexylA analyte while also suppressing the less nonpolar TethylA analyte. When analyzing the same solution in the femtoESI mode, the two analytes become more unequal in relative intensity (Figure 3b top). This is complemented by a decrease in the TIC signal by 3+ orders of magnitude and an increase to the maximum IT of 8000 ms (Figure 3). Also shown in Figure 3a are the relative signal stabilities for the two modes. The nanoESI mode is much more stable and produces about 10^6–10^7 ions per scan. The femtoESI mode appears to have a higher degree of signal variability with scans containing 10^0–10^2 ions per scan and other scans detect zero ions, a result of signal instability when operating in the femtoESI mode.

The relatively higher ThexylA to TethylA ion signal is attributed to the longer alkyl chain length in association which increases surface activity and nonpolar characteristics. Ions with a higher surface activity tend to have increased propensities for positions along the exterior of the charged droplets during the evaporation/fission processes based on the ion evaporation model (IEM)[8,28] and thus yield more intense signals.

High-frequency current measurements were collected at a 1000 Hz sampling rate on our electrometer. These data show that the femtoESI current is continuous at the lower end of the femtoESI mode and reveals low frequency pulsing modes near the onset of the nanoESI mode. This pulsing phenomenon has been revealed especially for the 10 TΩ resistor where the upper end of the femtoESI mode and the nanoESI mode show pulsing modes which increase in duty cycle with increasing applied voltage (Figure S11). There have not been any data observed for a high frequency pulsing mode.

Ionization of a Peptide Mixture. One of the more attractive routes for characterizing and applying the femtoESI mode is its

https://doi.org/10.1021/jasms.2c00369
J. Am. Soc. Mass Spectrom. 2023, 34, 913−921

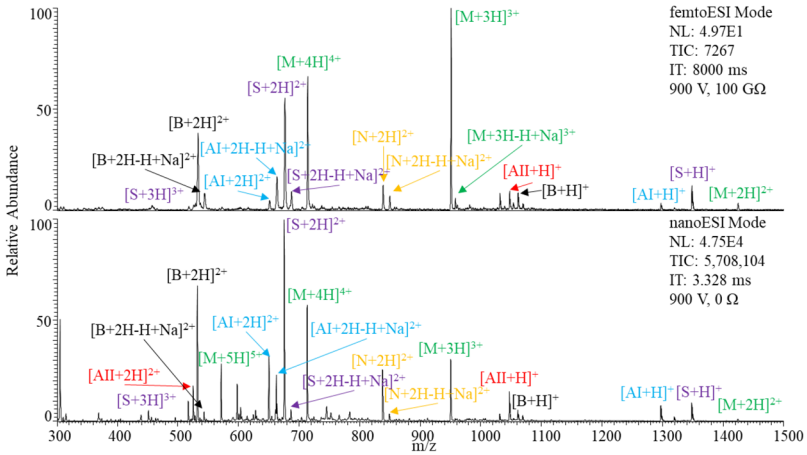

Figure 4. Mass spectrum for an aqueous 10 μM equimolar peptide mixture (angiotensin I (AI, blue), angiotensin II (AII, red), substance P (S, purple), bradykinin (B, black), melittin (M, green), and neurotensin (N, yellow)) analyzed under the femtoESI (top) and nanoESI (bottom) modes with or bypassing a 100 GΩ resistor at 900 V.

perceived effect on improving IE of analytes in a mixture. The perceived increase in IE is thought to be caused by the decreased droplet size of the femtoESI mode as a result of decreasing solution flow rate.[2,3,6−8,10−12,34] Sufficiently small droplets approach the statistical likelihood that each droplet formed will contain ≤1 analyte at a bulk solution concentration of ∼10 μM, meaning that under charge residue model (CRM) conditions more of the droplet charge will be imparted on a single analyte leading to more efficient charging. To achieve these conditions, droplets formed will need to have a radius of ∼30 nm, which has been hypothesized to be of the magnitude generated by femtoESI.[2] Based on previous studies by Rahman et al, flow rate has a large impact on the optimal overall and charge state signal attainable for each analyte where there is an optimal flow rate for each analyte of the mixture.[35] To reach this level of optimization, further instrumentation development is needed for femtoESI.

A mixture of peptides was also analyzed with alternating femtoESI and nanoESI modes. This equimolar mixture contains angiotensin I, angiotensin II, substance P, bradykinin, melittin, and neurotensin (Figure 4). For this mixture, the nanoESI mode (bottom) has been shown to favor the ionization of substance P $[S + 2H]^{2+}$ and bradykinin $[B + 2H]^{2+}$.[7,36] When shifting from the nanoESI mode to the femtoESI mode, an increase in the intensity of melittin peaks $[M + 3H]^{3+}$ is observed which is consistent with previously published results and was attributed to lower solution flow rate and initial droplet size (Figure 4 top).[7,36] Of the peaks for melittin in the nanoESI mode which are observed, the average charge state (ACS) is higher than in the femtoESI mode. This is another factor supporting the femtoESI mode as a softer ionization source compared to that of the nanoESI mode.

The nanoESI mode (Figure 4 bottom) shows an affinity toward the ionization of substance P and suppression of the melittin peak distribution.[7,36] The femtoESI mode (Figure 4 top) shows a perceived change in the IE with a large increase in the intensity of melittin and a decrease in substance P relative intensity. Melittin shows an overall decrease in the ACS in the femtoESI mode (3.37) compared to nanoESI (3.97). The increase in ACS in the nanoESI can be mostly attributed to the large increase in 3+ charge state intensity for the nanoESI mode, as well as the increase in the CSD for nanoESI with the appearance of a 5+ charge state. The transition from the nanoESI mode to the femtoESI mode for the peptide mixture also leads to a 3 order of magnitude change in TIC, NL, and IT.

An analysis of the amino acid (AA) composition for the peptides has been considered a method of characterizing and rationalizing the IE of oligopeptides.[26] Liigand et al. reports that although there is a correlation between log IE and size, the benefits of additional AA residues drops off after 5, leading to the AA composition being more relevant than the size.[25]

The AA residue composition for the oligopeptide is thought to be the most impactful on the log IE of the entire peptide (Table S3).[25] Melittin lacks Phe and His residues which are among the AAs with the highest ionization efficiencies and volumes. It also contains four Leu residues which is the AA with the highest IE. This could be why melittin's ionization behavior is capable of change for different spray modes.

It also has three Gly and two Ala residues which are hydrophilic and have small volumes which also are indicators of signal suppression.[25] Neurotensin lacks the IE boosting Phe and His residues but contains two Leu residues, which is the AA with the highest IE. Substance P has two Phe and one Leu residues which aid in enhancing the IE to the highest observed in Figure 4. Bradykinin benefits from two Phe residues which help make up for its smaller size, giving bradykinin the second most intense nanoESI peak. By evaluating the characteristically IE boosting and suppressing AAs present in the analytes, some of the relative intensity and charging behavior of the peptides in the mass spectrum can be evaluated.

One parameter of the peptides shown in Table S2 is the net charge of the peptide at neutral pH. In the femtoESI mode (Figure 4 top), the relative intensities of analytes follow the trend of solution net charge. Angio I and II have the lowest neutral pH net charges and have the lowest relative intensity in the femtoESI mode. Each of the following increases in net charge of the peptide in solution comes with an increase in the relative intensity observed in the mass spectrum, ending with melittin as the most intense and highest net charge analyte. Since the net charge of analytes in solution is a direct result of the AA residue makeup of the peptide, the trends in relative intensities of each analyte can be rationalized by the chemical and physical characteristics of the peptide.

https://doi.org/10.1021/jasms.2c00369
J. Am. Soc. Mass Spectrom. 2023, 34, 913−921

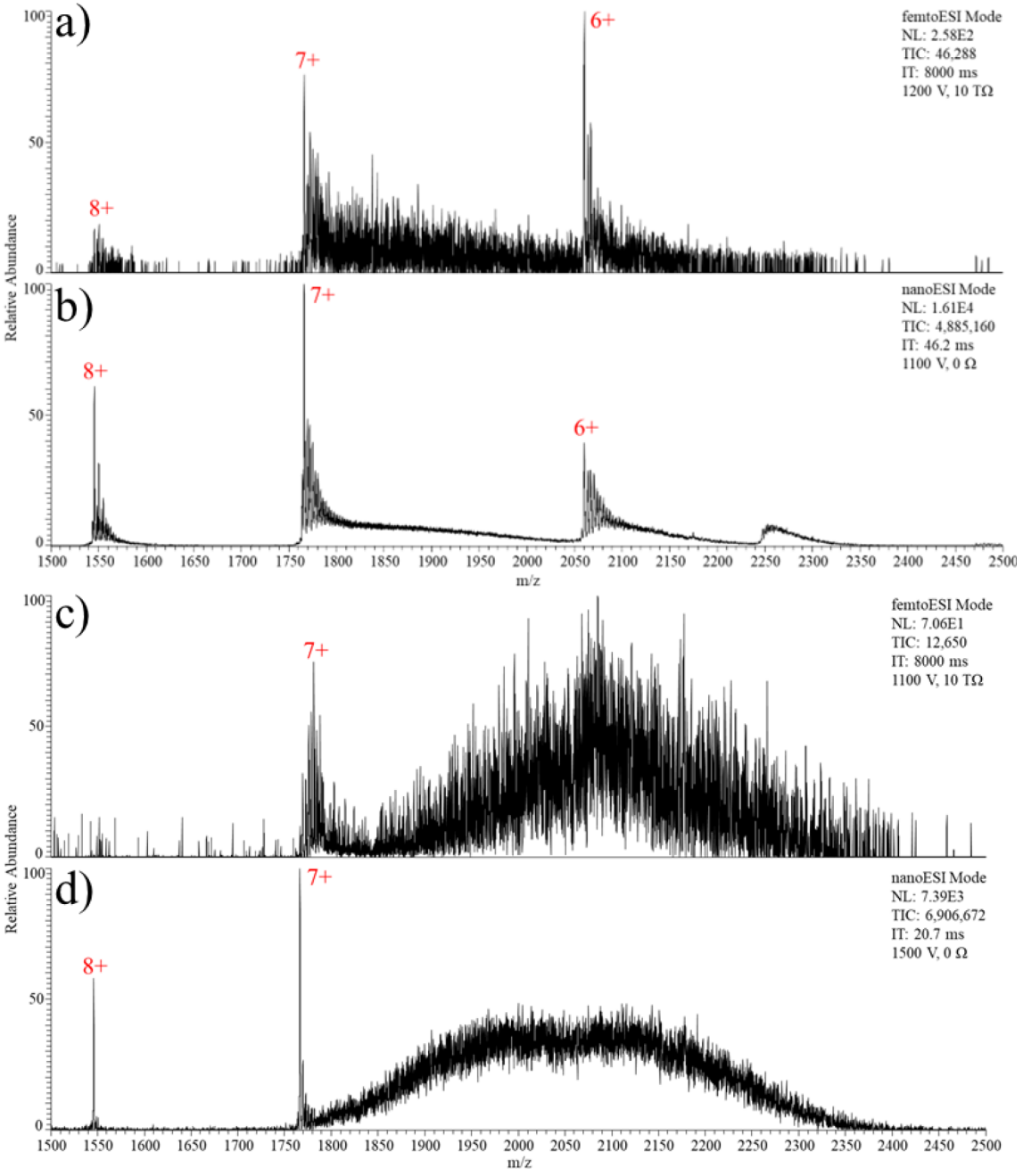

Figure 5. Mass spectrum of 10 μM cytochrome *c* in (a, b) 100 μM ammonium acetate and (c, d) 100 μM ammonium acetate with 1 mM NaCl. Each solution is analyzed via femtoESI (a, c) and nanoESI (b, d) spray modes. Current values for spectra a−d are 56.2 pA, 10.4 nA, 19.8 pA, and 138 nA, respectively.

Figure 4 also shows evidence of an interesting femtoESI phenomenon, that being the increase in sodiated peaks in the femtoESI mode compared to the nanoESI mode. This is observed for the angio I peaks where the sodiated 2+ peak in the nanoESI mode is less intense than the protonated 2+ peak, and after transitioning to the femtoESI mode, the sodiated peak is then the more intense peak. In all cases where a sodiated peak is observed, the sodiated peak is a single sodium adduct which is more relatively intense in the femtoESI mode than the nanoESI mode even when no salts are added to the working solutions. The femtoESI mode also enhances sodiated peaks for substance P, melittin, and neurotensin. The appearance of these sodiated peaks, especially in high relative intensity, is another suggestion that the femtoESI mode is operating to generate smaller initially charged droplets which evaporate to dryness during desolvation and cannot eject charge originating from salt ions from the droplets due to Rayleigh fission events. Instead, charge is retained on the droplet and salt ions adduct to the analyte during charging.[13] Since no sodium ions have been added to the sample solutions, the source of sodium ions was investigated. Sodium ions originating from the DI water used for dilutions has been ruled out due to type I HPLC water requiring sodium concentrations of <1 ppb to pass qualifications. A sodium concentration of <1 ppb corresponds to less than one sodium ion per droplet for 100 nm initial droplets. Impurities found in

https://doi.org/10.1021/jasms.2c00369
J. Am. Soc. Mass Spectrom. 2023, 34, 913−921

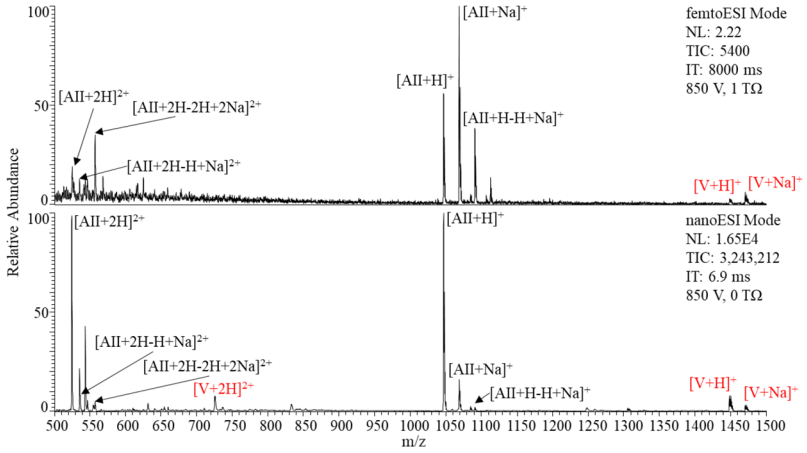

Figure 6. Analysis of a glycan/peptide mixture of 10 μM vancomycin (V) and angiotensin II (AII) in a 1:1 methanol:water solution. The femtoESI mode (top) and the nanoESI mode (bottom) are shown with the resulting labeled vancomycin (red) and angiotensin II (black) peaks. The two modes are alternated via a 1 TΩ resistor and 850 V.

the sample could originate from the sample powder purified from solutions with high salt concentrations.[37] Another possible source of sodium ions is the borosilicate glass used to manufacture our emitters and used to spray solutions. Borosilicate emitters have been known to contain significant amounts (~4%) of Na_2O which is believed to contribute to sodium adduction in this case.[13,37]

Ionization of Proteins. Analysis for the femtoESI and nanoESI modes for the protein cytochrome *c* (cyt c) in the ammonium acetate and ammonium acetate with NaCl solutions shows some intensity changes in the resulting mass spectrum (Figure 5). NaCl has been spiked into solutions for Figure 5c,d to evaluate the effect of additional salt concentration in the femtoESI mode. The different salt adducts trends observed here suggest these cyt c charge states result from different ionization mechanisms.[38] Previous research has indicated the 8+ and 7+ peaks for cyt c are ionized via different charging mechanisms.[39] When alternating between femtoESI and nanoESI modes, we do observe some different trends for the salt adducts versus protonated peak relative intensities for these charge states. This has been observed across three cyt c samples (aqueous, ammonium acetate, ammonium acetate plus sodium chloride) (Figures 5 and S12). In general, the 7+ charge state tends to increase in salt adduction when scanning in the femtoESI mode; the 8+ peak appears to decrease in salt adduction for analysis in the femtoESI mode. For the cyt c in ammonium acetate, the nanoESI mode has an ACS of 7.11 and a CSD of 6^+–8^+. The femtoESI mode has a reduced ACS of 6.57 and has an identical CSD of 6^+–8^+. This decrease in ACS for the femtoESI mode can be rationalized by a protein which resists unfolding and stays trapped in the droplets, ionizing via the charge residue model (CRM).[39,40] The completely folded native protein has less surface area and exposed chargeable residues, so a lower ACS may be reflective of a softer ionization method that retains native protein structures. In addition to the typical isotopic peaks, there are several peaks with mass shifts corresponding to salt and sodium ($NaCl/Na^+$) adducts. Transitioning to the femtoESI mode for the ammonium acetate solution shows that the protonated peaks are still dominant, but the relative intensities of the sodiated peaks is increased for femtoESI.

For the sodium chloride spiked sample, a large salt cluster appears over the 1800–2400 *m/z* range in both spray modes and this salt cluster suppresses the signal of the cyt c 6+ peak. For operation in the nanoESI mode, only two cyt c charge states are observed, 7+ and 8+. The ACS (7.37) is higher for cyt c in the nanoESI mode versus the ACS of 7.00 in the femtoESI mode (Figure 5c,d). The addition of NaCl appears to influence the amount of sodium adduct observed in the femtoESI mode. While the protonated peaks are dominant for Figure 5a,b,d, there is a significant decrease in the relative intensity of protonated peak observed in Figure 5c.

Both modes operate to produce native mass spectra which correspond to previously reported data by Allen et al, with a native CSD for cyt c in the 6^+–8^+ range.[3,37] The data presented in Figure 5 also show that a relatively stable protein such as cyt c does not experience a large difference in charging for alternating between spray modes, an overall difference of about half an ACS, whereas our previous studies have reported ~1 ACS difference.[3]

Further analysis of the peaks observed in the mass spectra shows that each charge state is comprised of several peaks. These adduct peaks are both more intense, relative to the main peak for a given charge state, and more numerous in the femtoESI spectrum than the nanoESI spectrum even for an aqueous solution (Figure S12). This is a phenomenon not observed in our previous femtoESI work where a different sample of cyt c did not display any observable sodium adduct peaks in the femtoESI or nanoESI modes.[3] Figure S12 also repeats aqueous cyt c data from our previous work to generate a femtoESI ACS of 6.9.[3] The salt adduct phenomenon discussed for peptide charging also appears to apply to protein charging, where the femtoESI mode leads to an overall decrease in ion signal but an increase in charging due to sodium ion adducts.

Ionization of Glycan/Peptide Mixture. Two different classes of analytes (peptide and glycan) were analyzed together in an equimolar mixture (Figure 6). Literature and theory would suggest that the glycan, vancomycin, will be suppressed in the nanoESI mode due to its lower surface activity compared to the peptide (angiotensin II). During the transition to the femtoESI mode, the signal for vancomycin should be improved due to more equity in charging under the femtoESI mode. This trend follows from the paper from Li et

https://doi.org/10.1021/jasms.2c00369
J. Am. Soc. Mass Spectrom. 2023, 34, 913–921

al., who showed that the nanoESI mode favors the ionization and detection of angiotensin II but spraying in the low flow rate subchannel mode enhanced the vancomycin signal.[7]

On/off alternation of the femtoESI and nanoESI modes for the glycan/peptide mixture results in different signal intensities and charge distributions for the two analytes in the mixture. For the femtoESI mode, the angio II charge state has a more intense 1+ charge state where the sodiated peak is more intense than the protonated peak. There is a small 2+ peak for angio II which is almost hidden by the rising baseline in the lower mass region of the spectra. For the nanoESI mode, the dominating peaks for angio II are the protonated 2+ and 1+ peaks. There are also sodiated peaks in the nanoESI spectrum, but they are all less intense than their protonated counterparts. The 1+ peak for nanoESI also displays a protonated peak, which is now more intense than the sodiated peak. Peaks have been assigned labels to reflect that during the process of sodium adduction, the addition of an additional sodium comes with the loss of a proton.[41] This keeps the total charge constant and reflects a shift in mass.

Analyzing vancomycin in the femtoESI mode yields only two peaks, one protonated 1+ peak and one sodiated 1+ peak. Only one additional vancomycin peak is observed when alternating to the nanoESI mode, that being the 2+ protonated peak, but the vancomycin 1+ peak has protonated and sodiated peaks which swap in relative intensity, where the protonated peak is favored for the 1+ charge state. Sodiated peaks may be more intense in the femtoESI mode due to the small initially charged droplets which do not undergo as many Rayleigh fission events, which would reduce the salt concentration in the droplet through the ejection of charge. The higher vapor pressure of smaller droplets will facilitate the evaporation of HCl, thus enriching the less volatile Na^+ during droplet evaporation.[41] If the analyte in the droplet containing salt does not undergo fission and instead is allowed to evaporate to dryness with the analyte inside, then (part of) the charge imparted onto the analyte would originate from sodium ions because the excess charge from sodium cannot be ejected from the droplet via Rayleigh fission.

CONCLUSIONS

The applied voltage range accessible to the femtoESI mode has been expanded by the utilization of large resistors. It has been found that the femtoESI mode applied voltage range is expanded from 100 V (0 Ω) to 1400 V (100 TΩ). For the first time a 100 TΩ resistor has been assembled and evaluated for use in an ESI circuit. This 100 TΩ resistor produces the largest femtoESI applied voltage range of any of the resistors tested while still producing mass spectrometer and current signals. This femtoESI applied voltage range expansion has been shown to be applicable for various classes of analytes, ranging from tetraalkylammonium salts, peptides, and glycans, as well as protein analysis in aqueous solutions. The performances of analyzing a peptide mixture in the femtoESI mode are demonstrated as the enhancement of melittin and sodiated peaks. The increase in relative intensity of sodiated peaks in the mass spectrum suggests more evaporative drying, which could occur when smaller initially charged droplets undergo no or less Rayleigh fission events.

There has also been a shift in ACS and CSD of multiply charged species when alternating between the two ESI modes of interest. Analytes (melittin, cyt c, etc.) are generally shifted toward lower ACS when transitioning from the nanoESI mode to the femtoESI mode, maintaining the position that the femtoESI mode is a softer method of ionization compared to the nanoESI mode.

ASSOCIATED CONTENT

Supporting Information

The Supporting Information is available free of charge at https://pubs.acs.org/doi/10.1021/jasms.2c00369.

(PDF)

AUTHOR INFORMATION

Corresponding Author

Anyin Li − *Department of Chemistry, University of New Hampshire, Durham, New Hampshire 03824, United States;* orcid.org/0000-0003-0291-5688; Email: anyin.li@unh.edu

Authors

Nicholas Allen − *Department of Chemistry, University of New Hampshire, Durham, New Hampshire 03824, United States*

Huishan Li − *Department of Chemistry, University of New Hampshire, Durham, New Hampshire 03824, United States*

Taoqing Wang − *Department of Chemistry, University of New Hampshire, Durham, New Hampshire 03824, United States*

Complete contact information is available at: https://pubs.acs.org/10.1021/jasms.2c00369

Author Contributions

Nicholas Allen: methodology, data collection, investigation, formal analysis, writing of original draft, reviewing and editing of manuscript. Huishan Li: investigation, data collection, formal analysis, reviewing and editing of manuscript. Taoqing Wang: formal analysis, reviewing and editing of manuscript. Anyin Li: conceptualization, funding acquisition, project administration, reviewing and editing of manuscript.

Notes

The authors declare no competing financial interest.

ACKNOWLEDGMENTS

This material is based upon work supported by the Chemical Measurement and Imaging program in the National Science Foundation Division of Chemistry under Grant CHE-2203289 and funding from the Established Program to Stimulate Competitive Research.

REFERENCES

(1) Kebarle, P.; Tang, L. From Ions in Solution to Ions in the Gas-Phase - the Mechanism of Electrospray Mass-Spectrometry. *Anal. Chem.* **1993**, *65* (22), 972A−986A.

(2) Li, H.; et al. Conducting and characterizing femto flow electrospray ionization. *Analyst* **2022**, *147* (6), 1071−1075.

(3) Allen, N. R.; et al. Femtoamp and picoamp modes of electrospray and paper spray ionization. *Int. J. Mass Spectrom.* **2021**, *469*, 116696.

(4) Wang, T.; et al. Ultra-low current electrospray ionization of chloroform solution for the analysis of perfluorinated sulfonic acids. *Rapid Commun. Mass Spectrom.* **2023**, e9501.

(5) Rahman, M.; Wu, D.; Chingin, K. Direct Analysis of Aqueous Solutions and Untreated Biological Samples Using Nanoelectrospray Ionization Mass Spectrometry with Pipette Tip in Series with High-Ohmic Resistor as Ion Source. *J. Am. Soc. Mass Spectrom.* **2019**, *30* (5), 814−823.

(6) Susa, A. C.; Xia, Z.; Williams, E. R. Small Emitter Tips for Native Mass Spectrometry of Proteins and Protein Complexes from Nonvolatile Buffers That Mimic the Intracellular Environment. *Anal. Chem.* **2017**, *89* (5), 3116−3122.
(7) Li, M.; et al. Nested-channel for on-demand alternation between electrospray ionization regimes. *Chem. Sci.* **2021**, *12* (5), 1907−1914.
(8) Konermann, L.; et al. Unraveling the mechanism of electrospray ionization. *Anal. Chem.* **2013**, *85* (1), 2−9.
(9) Li, Y.; Cole, R. B. Shifts in peptide and protein charge state distributions with varying spray tip orifice diameter in nano-electrospray Fourier transform ion cyclotron resonance mass spectrometry. *Anal. Chem.* **2003**, *75* (21), 5739−46.
(10) Crotti, S.; Seraglia, R.; Traldi, P. Some thoughts on electrospray ionization mechanisms. *Eur. J. Mass Spectrom (Chichester)* **2011**, *17* (2), 85−99.
(11) Wilm, M.; Mann, M. Analytical properties of the nano-electrospray ion source. *Anal. Chem.* **1996**, *68* (1), 1−8.
(12) Schmidt, A.; Karas, M.; Dulcks, T. Effect of different solution flow rates on analyte ion signals in nano-ESI MS, or: when does ESI turn into nano-ESI? *J. Am. Soc. Mass Spectrom.* **2003**, *14* (5), 492−500.
(13) Kenderdine, T.; et al. Submicrometer Nanospray Emitters Provide New Insights into the Mechanism of Cation Adduction to Anionic Oligonucleotides. *Anal. Chem.* **2018**, *90* (22), 13541−13548.
(14) Smith, R. D.; Shen, Y.; Tang, K. Ultrasensitive and quantitative analyses from combined separations-mass spectrometry for the characterization of proteomes. *Acc. Chem. Res.* **2004**, *37* (4), 269−78.
(15) Susa, A. C.; et al. Submicrometer Emitter ESI Tips for Native Mass Spectrometry of Membrane Proteins in Ionic and Nonionic Detergents. *J. Am. Soc. Mass Spectrom.* **2018**, *29* (1), 203−206.
(16) Susa, A. C.; et al. Charging of Proteins in Native Mass Spectrometry. *J. Am. Soc. Mass Spectrom.* **2017**, *28* (2), 332−340.
(17) Wang, H.; Ouyang, Z.; Xia, Y. Peptide fragmentation during nanoelectrospray ionization. *Anal. Chem.* **2010**, *82* (15), 6534−41.
(18) Pfeifer, R. J.; Hendricks, C. D. Parametric Studies of Electrohydrodynamic Spraying. *AIAA J.* **1968**, *6* (3), 496.
(19) Ikonomou, M. G.; Blades, A. T.; Kebarle, P. Electrospray Ion Spray - a Comparison of Mechanisms and Performance. *Anal. Chem.* **1991**, *63* (18), 1989−1998.
(20) Ninomiya, S.; Hiraoka, K. Pulsed Nano-Electrospray Ionization with a High Voltage (4000 V) Pulse Applied to Solutions in the Range of 200 ns to 1 ms. *J. Am. Soc. Mass Spectrom.* **2020**, *31* (3), 693−699.
(21) Kiontke, A.; Oliveira-Birkmeier, A.; Opitz, A.; Birkemeyer, C. Electrospray Ionization Efficiency Is Dependent on Different Molecular Descriptors with Respect to Solvent pH and Instrumental Configuration. *PLoS One* **2016**, *11*, e0167502.
(22) Leito, I.; et al. Towards the electrospray ionization mass spectrometry ionization efficiency scale of organic compounds. *Rapid Commun. Mass Spectrom.* **2008**, *22* (3), 379−84.
(23) Smith, R. D.; Shen, Y. F.; Tang, K. Q. Ultrasensitive and quantitative analyses from combined separations-mass spectrometry for the characterization of proteomes. *Acc. Chem. Res.* **2004**, *37* (4), 269−278.
(24) Oss, M.; et al. Electrospray ionization efficiency scale of organic compounds. *Anal. Chem.* **2010**, *82* (7), 2865−72.
(25) Liigand, P.; et al. Think Negative: Finding the Best Electrospray Ionization/MS Mode for Your Analyte. *Anal. Chem.* **2017**, *89* (11), 5665−5668.
(26) Liigand, P.; Kaupmees, K.; Kruve, A. Influence of the amino acid composition on the ionization efficiencies of small peptides. *J. Mass Spectrom* **2019**, *54* (6), 481−487.
(27) Page, J. S.; et al. Ionization and transmission efficiency in an electrospray ionization-mass spectrometry interface. *J. Am. Soc. Mass Spectrom.* **2007**, *18* (9), 1582−90.
(28) Cech, N. B.; Enke, C. G. Practical implications of some recent studies in electrospray ionization fundamentals. *Mass Spectrom Rev.* **2001**, *20* (6), 362−87.
(29) Usmanov, D. T.; et al. Electrospray Generated from the Tip-Sealed Fine Glass Capillary Inserted with an Acupuncture Needle Electrode. *J. Am. Soc. Mass Spectrom.* **2018**, *29* (12), 2297−2304.
(30) Wei, Z.; et al. Pulsed Direct Current Electrospray: Enabling Systematic Analysis of Small Volume Sample by Boosting Sample Economy. *Anal. Chem.* **2015**, *87* (22), 11242−8.
(31) Alexander, M. S.; Paine, M. D.; Stark, J. P. Pulsation modes and the effect of applied voltage on current and flow rate in nanoelectrospray. *Anal. Chem.* **2006**, *78* (8), 2658−64.
(32) Arscott, S.; Troadec, D. Electrospraying from nanofluidic capillary slot. *Appl. Phys. Lett.* **2005**, *87* (13), 134101.
(33) Hiraoka, K.; et al. Development of probe electrospray using a solid needle. *Rapid Commun. Mass Spectrom.* **2007**, *21* (18), 3139−44.
(34) Li, Y.; Cole, R. B. Shifts in Peptide and Protein Charge State Distributions with Varying Spray Tip Orifice Diameter in Nano-electrospray Fourier Transform Ion Cycltron Resonance Mass Spectrometry. *Anal. Chem.* **2003**, *75*, 5739.
(35) Rahman, M. M.; Wu, D.; Chingin, K. Correction to: Direct Analysis of Aqueous Solutions and Untreated Biological Samples Using Nanoelectrospray Ionization Mass Spectrometry with Pipette Tip in Series with High-Ohmic Resistor as Ion Source. *J. Am. Soc. Mass Spectrom.* **2019**, *30* (7), 1337−1337.
(36) Marginean, I.; et al. Picoelectrospray ionization mass spectrometry using narrow-bore chemically etched emitters. *J. Am. Soc. Mass Spectrom.* **2014**, *25* (1), 30−6.
(37) Nguyen, G. T. H.; et al. Nanoscale Ion Emitters in Native Mass Spectrometry for Measuring Ligand-Protein Binding Affinities. *ACS Cent Sci.* **2019**, *5* (2), 308−318.
(38) Pimlott, D. J. D.; Konermann, L. Using covalent modifications to distinguish protein electrospray mechanisms: Charged residue model (CRM) vs. chain ejection model (CEM). *Int. J. Mass Spectrom.* **2021**, *469*, 116678.
(39) Aliyari, E.; Konermann, L. Formation of Gaseous Proteins via the Ion Evaporation Model (IEM) in Electrospray Mass Spectrometry. *Anal. Chem.* **2020**, *92* (15), 10807−10814.
(40) Pimlott, D. J. D.; Konermann, L. Using covalent modifications to distinguish protein electrospray mechanisms: Charged residue model (CRM) vs. chain ejection model (CEM). *Int. J. Mass Spectrom.* **2021**, *469*, 116678.
(41) Hiraoka, K.; et al. Comparative study of H3O+ (aq) and NH4+ (aq) on electrophoresis, protonating ability, and sodiation of proteins. *Int. J. Mass Spectrom.* **2022**, *471*, 116728.

https://doi.org/10.1021/jasms.2c00369
J. Am. Soc. Mass Spectrom. 2023, 34, 913−921